Talanta 99 (2012) 512–519

Contents lists available at SciVerse ScienceDirect

Talanta

journal homepage: www.elsevier.com/locate/talanta

Magnetic graphene nanosheets based electrochemiluminescence immunoassay of cancer biomarker using CdTe quantum dots coated silica nanospheres as labels

Fang Liu [a], Yan Zhang [a], Shenguang Ge [b], Juanjuan Lu [a], Jinghua Yu [a,*], Xianrang Song [c,**], Su Liu [d]

[a] Key Laboratory of Chemical Sensing & Analysis in Universities of Shandong (University of Jinan), School of Chemistry and Chemical Engineering, University of Jinan, Jinan 250022, PR China
[b] Shandong Provincial Key Laboratory of Fluorine Chemistry and Chemical Materials, University of Jinan, Jinan 250022, PR China
[c] Cancer Research Center, Shandong Tumor Hospital, Jinan 250012, PR China
[d] School of Medicine and Life Sciences, University of Jinan, Jinan 250022, PR China

ARTICLE INFO

Article history:
Received 27 March 2012
Received in revised form
5 June 2012
Accepted 9 June 2012
Available online 26 June 2012

Keywords:
Electrochemiluminescence
Magnetic graphene nanosheets
CdTe quantum dots coated silica nanospheres
Sandwich-type immunosensor

ABSTRACT

A highly sensitive electrochemiluminescence (ECL) immunosensor for the detection of prostate specific antigen (PSA) was designed using biofunctionalized magnetic graphene nanosheets ($G@Fe_3O_4$) as immunosensing probes and CdTe quantum dots coated silica nanospheres (Si/QDs) as signal amplification labels. In this work, a sandwich-type immunosensor was fabricated, which was assembled on the surface of indium tin oxide glass (ITO). The analyte was detected in a home-made flow injection ECL (FI-ECL) cell through the immunosensor. Owing to the signal amplification of $G@Fe_3O_4$ composite and Si/QDs, the ECL measurement showed a great increase in detection signals compared with the unamplified method. Under optimal conditions, a wide detection range (0.003–50 ng mL^{-1}) and a low detection limit (0.72 pg mL^{-1}) were obtained through the sandwich-type immunosensor. The proposed strategy successfully demonstrated a reproducible, specific, and potent method that can be expanded to detect other proteins.

1. Introduction

Tumor marker molecules occur in blood and tissues that are associated with cancer, and whose identification and determination are significant in patient diagnosis and clinical therapy [1,2]. As a result, the detection of tumor markers has attracted a lot of scientific workers' attention. Recently, various immunoassays have been reported to realize the determination of tumor markers [3–5]. Common approaches have been utilized for immunoassays, including enzyme-linked immunosorbent assay [6], chemiluminescence immunoassay [7], fluorescence immunoassay [8], electrochemical immunoassay, electrochemiluminescence immunoassay, quartz crystal microbalance immunoassay, and surface plasmon resonance immunoassay. Further researches have been developed for the enhancement of detection sensitivity by signal amplification or employment of different detection technologies [9]. Successful signal amplification strategies include applying new redox-active probes, coupling amplification-by-polymerization concepts with electrochemical detection, integrating enzyme-assisted signal amplification processes, and incorporating nanomaterials to increase loading of tags, etc. [10–13]. Among these methods, electrochemiluminescence immunoassay has become one of the predominant analytical techniques, owing to its high sensitivity, simple instrumentation, low cost, and good compatibility with advanced micromachining technologies. In spite of some advances in this field, it is still a challenge to explore new protocols and strategies for the further improvement of the sensitivity and the lower detection limit. Magneto-controlled molecular bioelectronics has become a new tool for monitoring biomolecules in food, environment, and clinical samples [14]. As reported in the preceding literature [15], batch-type magnetic separators have been fabricated on a single chip for trapping and directed sequential elution of magnetic particles in flowing fluids. But, some weaknesses exist in magnetic particles, such as the limited capture capacity toward the antigen in the sample and the damage to the biological macromolecules to some degrees. In this paper, we proposed a new hybrid nanomaterial by making magnetic nanoparticles to assemble onto the graphene nanosheets. The strong magnetic attribute of $G@Fe_3O_4$ offers significant use for biomagnetic separations, as the carriers for targeted analytes. The solubility and versatility of the $G@Fe_3O_4$ pave the way for the fabrication of multifunctional composites through the

* Corresponding author. Tel.: +86 531 82767161.
** Corresponding author. Tel.: +86 531 82767161.
E-mail addresses: ujn.yujh@gmail.com (J. Yu), sxr@vip.163.com (X. Song).

0039-9140/$ - see front matter © 2012 Elsevier B.V. All rights reserved.
http://dx.doi.org/10.1016/j.talanta.2012.06.021

convenient solution-processing technique. The multifunctional G@Fe_3O_4 could serve as a new kind of promising nanofiller to produce high-performance composites and coatings with both electrical and magnetic properties. And the scraggy nanostructures could provide a large surface area for the immobilization of biomolecules. In short, these hybrid nanomaterials possess so many advantages, such as, excellent separation function, high electrical conductivity, high surface-to-volume ratio, and good biocompatibility, which are far better than those of the magnetic particle and the graphene nanosheet.

With the use of the flow-through us system, assembled with the home-made ECL monitoring cell, trapping magnetic graphene nanosheets as the carriers for the corresponding PSA–primary antibodies (G@Fe_3O_4–Ab_1) could efficiently capture the analytes, because of the large surface area of the nanosheets. Moreover, to further amplify the ECL performance and achieve much higher sensitivity, we employ Si/QDs as signal tags to increase CdTe QDs loading per immunoreaction in comparison with single QDs [16,17], which have been used as ECL and luminescence labels for bioassays and bioimages [18,19]. Another improvement is that the strategy could enhance the stability, precision, and reproducibility of the resultant immunosensors via lightening, even refraining the QDs from agglomeration, a common problem that occurs when using small nanoparticles as biological labels. Herein, we use this highly modified ECL reagent to label PSA–secondary antibody (Si/QDs–Ab_2), through the bioconjugation during the cross-linking reaction.

In this paper, we have designed a modified sandwich-type immunosensor with more advantages in contrast to the simple sandwich-type immunosensors that have been reported by some groups [20–22]. The infrequent magnetic graphene-based immunosensing probes could not only promote washing after synthesis with good biocompatibility, but also facilitate the electronic transfer and enhance the detection signals to a large extent. The method, in which using Si/QDs as signal labels to amplify the ECL signal, is also an advantage compared to that using single QDs. The modified sandwich-type immunoassay allows monitoring of the quantity of antigen via the ECL signal by cyclic voltammetry (CV) measurement, which shows high sensitivity, good compatibility and practical applicability. And it is predictable that this high-efficiency strategy has vast potential to be used in other biological assays.

2. Materials and methods

2.1. Reagents

All reagents were of analytical-reagent grade or the highest purity available and directly used for the following experiments without further purification and the aqueous solutions unless indicated were prepared with Milli-Q water (Millipore, USA). ITO (thickness of ITO layer: 150 nm; resistance < 15 Ω/square; thickness of glass: 1.1 mm) was obtained from Xiamen ITO Photoelectricity Industry (Xiamen China). Thionine (TH) was obtained from Acros. Anhydrous iron (III) chloride ($FeCl_3$, 98%), diethylene glycol (DEG, 99%), thioglycolic acid (TGA), 3-aminopropyl triethoxysilane (APTES), N-(3-dimethylaminopropyl)-N′-ethylcarbodiimide-hydro-chloride (EDC) and N-hydroxysuccinimide (NHS) were purchased from Alfa Aesar China Ltd. PSA, Ab_1, PSA–secondary antibody (Ab_2) and bovine serum albumin (BSA) were purchased from Shanghai Linc-Bio Science Co. Ltd (Shanghai Linc-Bio Science Co. Ltd. China). The washing buffer was PBS (0.01 M, pH 7.4), and 0.01 M PBS of various pH's prepared by adjusting the ratio of Na_2HPO_4 to NaH_2PO_4, containing 1.0 mM Na_2SO_3, was used as the electrolyte in the measuring system. The clinical serum samples were provided by Shandong Tumor Hospital.

2.2. Apparatus

The ECL experiments were carried out on an MPI-B multiple-parameter chemiluminescence analytical testing system equipped with an MPI-A/B multifunction chemiluminescence detector (Xi'An Remax Electronic Science & Technology Co. Ltd. Xi'an, Changchun Institute of Applied Chemistry Chinese Academy Sciences, China) at room temperature. The photoluminescence (PL) spectra were obtained on an RF-5301 spectrofluorometer (P.C. Shimadzu, Japan). Ultraviolet—visible (UV–vis) absorption spectra were recorded on a UV-2550 spectrophotometer (Shimadzu, Japan). Scanning electron microscope (SEM) images and energy dispersive spectrometer (EDS) were obtained using a JSM-6700F microscope (JEOL, Japan). Transmission electron microscope (TEM) images were obtained from a JEOL JEM-1400 microscope (JEOL, Japan).

2.3. Fabrication of the FI-ECL cell

The FI-ECL cell (Scheme 1) was fabricated by a cylindrical poly(methyl methacrylate) (PMMA). ITO slide glass (1.0 cm i.d.) was used as working electrode (WE). The FI-ECL cell mainly consisted of an ITO WE, two flow tubes, platinum counter electrode (CE), and Ag/AgCl reference electrode (RE). The WE, two flow tubes, CE, and RE were slided together by screws to form the airtight FI-ECL cell. Inlet and outlet were designed on the slide surface of the cell, which were nearly in a straight line with the ITO glass slide, and a flared opening was designed in the front of outlet. A round optical window was made at the bottom of the cell and light from the ECL reaction was transmitted through with the ITO coated glass electrode and detected by a photomultiplier tube (PMT) positioned below the cell. In addition, there is a vacant space for magnet at the bottom. The magnet was placed there in case of need.

2.4. Synthesis of magnetic graphene nanosheets (G@Fe_3O_4)

G@Fe_3O_4 were synthesized according to the literature [23] with a slight modification. Typically, NaOH (200 mg) was added into DEG (20 mL), heated at 120 °C for 1 h under N_2, and cooled down to 70 °C to produce a NaOH/DEG stock solution (10 mg mL^{-1} NaOH). Graphene oxide (GO) (30 mg) (synthesized from graphite using a

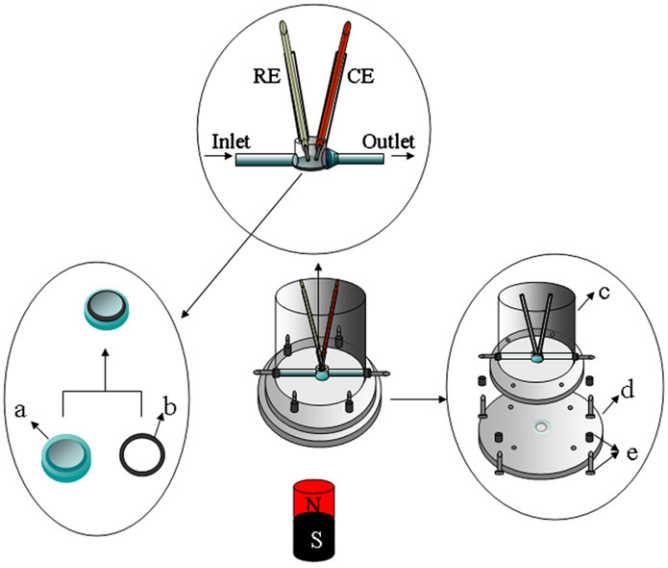

Scheme 1. Schematic diagram of the FI-ECL cell. RE: reference electrode; CE: counter electrode; (a) ITO slide glass; (b) airtight rubber; (c) top perspex block; (d) bottom perspex disk; (e) screw.

method mentioned in the literature [24]) was separated by centrifugation from GO aqueous solution (16,000 rpm, 5 min), redispersed in DEG (20 mL), and sonicated for 1 h. Then, $FeCl_3$ (120 mg) was added and stirred for 1 h. The above mixture was heated to 220 °C for 30 min under N_2 flow and constant stirring. Afterward, 5 mL of DEG stock solution at 70 °C was added rapidly into the hot mixture and further heated for another 1 h at 220 °C. The final products of G@Fe_3O_4 were separated by centrifugation and washed with ethanol for four times. Dry G@Fe_3O_4 magnetic powders were obtained by drying the residue at 60 °C in vacuum.

2.5. Synthesis of large monodispersed silica microspheres

Monodispersed silica nanospheres, used as carriers for QDs and Ab_2 immobilization, were synthesized according to the previously reported method [25] with a light modification. Initially, water (4.0 mL), ethanol (10.0 mL) and NH_3H_2O (2.0 mL) were loaded in the semi-batch reactor. Then, 100 μL of a TEOS solution was introduced into the system. In order to be well-distributed, the mixture was subjected to a vigorous mechanical stirring until it reached equilibrium at room temperature. Finally, the precipitated spherical silica particles were separated by centrifugation and washed with ethanol for five times. Dry silica nanospheres were obtained by drying the residue at 80 °C in vacuum.

2.6. Preparation of CdTe QDs functionalized silica nanospheres (Si/QDs)

The preparation of the water-soluble CdTe QDs was reported previously [26]. Herein, we took a method similar to that involved in the article mentioned above. In brief, 0.1980 g of $CdCl_2 \cdot 2.5H_2O$ was dispersed in 50 mL of water, and then 160 μL of TGA was added. The pH of the turbid suspension was adjusted to 11 by NaOH solution (1.0 M) to obtain a clear solution. The resulting solution was bubbled with highly pure N_2 for 30 min to form the CdTe precursors, and 10.0 mL of the NaHTe solution (obtained by the reaction of 0.1190 g $NaBH_4$ and 0.0492 g Te powder in oxygen-free water) was injected into the vigorously stirred solution immediately. The obtained QDs solutions were refluxed for different times to form different sizes of QDs by refluxing at 100 °C.

For the preparation of Si/QDs, 0.02 g of the prepared silica nanospheres were first dispersed in 2 mL of ethanol and treated with 0.4 mL of APTES. After stirring for 6 h, the suspension was centrifuged and washed with ethanol repeatedly for four times, and the amino-functionalized nanoparticles were obtained. Then, the amino-functionalized silica nanoparticles were dispersed in a mixture of CdTe QDs and EDC. The mixed suspension was stirred at 4 °C for 12 h. Unbound QDs were removed by successive centrifugation and washed with water several times. Finally, the as-prepared Si/QDs nanospheres, which had the same color as CdTe QDs themselves, were obtained and dispersed in water to a final volume of 1 mL.

2.7. Fabrication of the immunosensor

The ECL immunosensor was shown in Scheme 2. First, the as-prepared G@Fe_3O_4 (80 mg) was dispersed in 10 mL of PBS (pH∼7.4). After TH (1 mL, 1.0 mM) solution was added, the resulting mixture was set on a shaker at 37 °C for 48 h and then centrifuged. And the aminogroup of TH could attach onto the graphene through π–π stacking. After discarding the supernatant, the obtained product again was dispersed in 5 mL PBS. Then, 50 μL of GA (2.5%) was added into 0.5 mL of the G@Fe_3O_4/TH solutions and allowed to react for 1.0 h at room temperature. It can bridge the G@Fe_3O_4/TH and Ab_1 with covalent bond force. Then, the un-conjugated materials were washed away using PBS buffer with the aid of the magnet. Next, the Ab_1 (10 μL, 20 μg mL^{-1}) was bonded to the above compound by reacting with it for 60 min at 4 °C. Following that, the unbound antibodies were removed as the above mentioned method. Subsequently, the as-prepared G@Fe_3O_4/TH–GA–Ab_1 solution was mixed with 50 μL BSA (1 wt%), reacting for 1 h to block the nonspecific binding sites on the surface of G@Fe_3O_4/TH. At last, the obtained G@Fe_3O_4/TH–GA–Ab_1 only with specific binding sites was rinsed similarly, redispersed in PBS and stored at 4 °C when not in use.

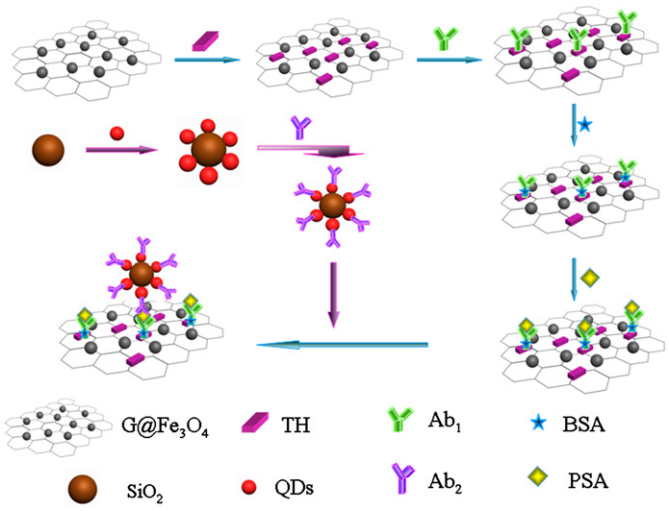

Scheme 2. Schematic representation of the fabrication of the ECL immunosensor with dual amplification strategy including both the fabrication of G@Fe_3O_4/TH–GA–Ab_1 and Ab_2–Si/QDs.

2.8. ECL detection of PSA with the immunosensor

10 μL of PSA solutions with different concentrations was mixed with the above immunosensor and the incubation was conducted at 4 °C for 1 h to make them react with the limited binding sites of Ab_1. Then the PSA immobilized G@Fe_3O_4/TH–GA–Ab_1 was obtained through the antigen–antibody specific interaction on the surface of G@Fe_3O_4. After that, Si/QDs labeled Ab_2 conjugation (Si/QDs–Ab_2) (prepared by mixing Si/QDs, EDC, NHS, Ab_2) was added into the mentioned solutions and incubated for 80 min at 4 °C to construct the sandwich-type immunocomplex G@Fe_3O_4/TH–GA–Ab_1–Ag–Ab_2–Si/QDs. The excess Si/QDs–Ab_2 was washed out with the help of external magnet. The integrated fabrication process described above was conducted in a centrifugal tube with a small volume of 1.5 mL. Following that, the fabricated immunosensors were diluted in PBS containing 1.0 mM Na_2SO_3, and then the mixed solution was flowed into the home-made detection cell and assembled on the ITO surface drawing support from a magnet. At last, cyclic voltammetry (CV) was applied to conduct ECL.

3. Results and discussion

3.1. Characterization of the FI-ECL cell

In comparison with conventional ECL flow cells, the proposed ECL cell had several apparent advantages. The new ECL cell had overcome the drawbacks of the conventional ECL cells as follows. First, the new ECL cell had a very small dead volume. Therefore, the newly designed ECL cell would decrease the dilution of samples and thus improved the detection sensitivity for FI. Second, the new ECL flow cell had a very low IR drop (potential drop, product of current and resistance). In the new design

(Scheme 1), the RE and CE were set in the bulk solution, and only the WE was located in the narrow thin layer. The WE, CE, and RE were placed closely, resulting in a much lower IR drop. The outlet with an expanded exit was placed on the bottom of the cell in a straight line with the inlet, hence, the magnetic materials with bulk mass could be washed away easily. Third, the surface of the ITO WE was placed opposite to the transparent window, resulting in nearly 100% of the ECL emission to be generated on the surface of the WE which is being detected by PMT. And, the area of ITO WE was larger than that of the glassy carbon electrode or gold electrode. This kind of ECL detector has high sensitivity.

3.2. Characterization of magnetic graphene nanosheets (G@Fe_3O_4)

3.2.1. UV–vis and fluorescence characterization

Ethanol was used as solvent and UV–vis was used to characterize the formation of G@Fe_3O_4 from 200 nm to 700 nm wavelength range. As shown in Supporting information Fig. S-1A, a small blue shift of G@Fe_3O_4 was observed in contrast to that of the individual graphene. This suggested that graphene and Fe_3O_4 were combined with strong chemical bonds force, confirming the successful composite of graphene and Fe_3O_4. And in the PL spectra, when Fe_3O_4 and G@Fe_3O_4 were both in their best excitation wavelength, their respective maximal emission wavelengths were 400 nm and 429 nm, which can be seen from the Supporting information Fig. S-1B. Apparently, the red shift phenomenon also demonstrated this combination powerfully. The next procedures were based on this composite.

3.2.2. TEM characterization

Fig. 1B shows typical TEM images of the synthesized G@Fe_3O_4. Compared with pure graphite (Fig. 1A), many nanoparticles could be observed on G@Fe_3O_4. The graphene nanosheets provided a large surface area for the assembly of the magnetic nanoparticles at the top and the bottom of nanosheets. Moreover, the synthesized graphene nanosheets and G@Fe_3O_4 could be homogeneously dispersed in the ethanol. Although most of the magnetite particles were uniformly distributed on the reduced GO sheets, a small quantity of magnetic nanoparticles were aggregated slightly due to the loading degree close to saturation. The external morphology of graphene and G@Fe_3O_4 dispersed in ethanol are shown in Fig. 1C and E, respectively, and some differences were observed. The magnetic components of G@Fe_3O_4 render mobility under an external magnetic field. When a magnet is placed beside a bottle filled with G@Fe_3O_4 dispersed in ethanol, the G@Fe_3O_4 particles quickly move along the magnetic field and completely deposit near the magnet (Fig. 1D), demonstrating high magnetic sensitivity.

3.3. Characterization of silica microspheres and CdTe QDs functionalized silica microspheres (Si/QDs)

3.3.1. PL spectra

The PL spectra were performed to illustrate the formation of CdTe QDs and Si/QDs. As shown in Supporting information Fig. S-2, an obvious red shift was obtained and this may be ascribed to the carboxylic groups located on the surface of CdTe QDs bonding strongly to the amino-functionalized silica nanospheres in the presence of EDC as the linker.

3.3.2. SEM and TEM characterization

In addition, the preparation of silica nanospheres and QDs bonding with silica nanospheres was characterized by SEM, EDS and TEM. As shown in Fig. 2A, this indicates that the silica nanospheres with good shape were obtained successfully. And it can be confirmed that QDs were successfully bonded to the silica nanosphere from Fig. 2B. What's more, Fig. 2C D showed that the elements Cd and Te existed in site "1", but not in site "2". This fact also demonstrated the combination effectively. The TEM images

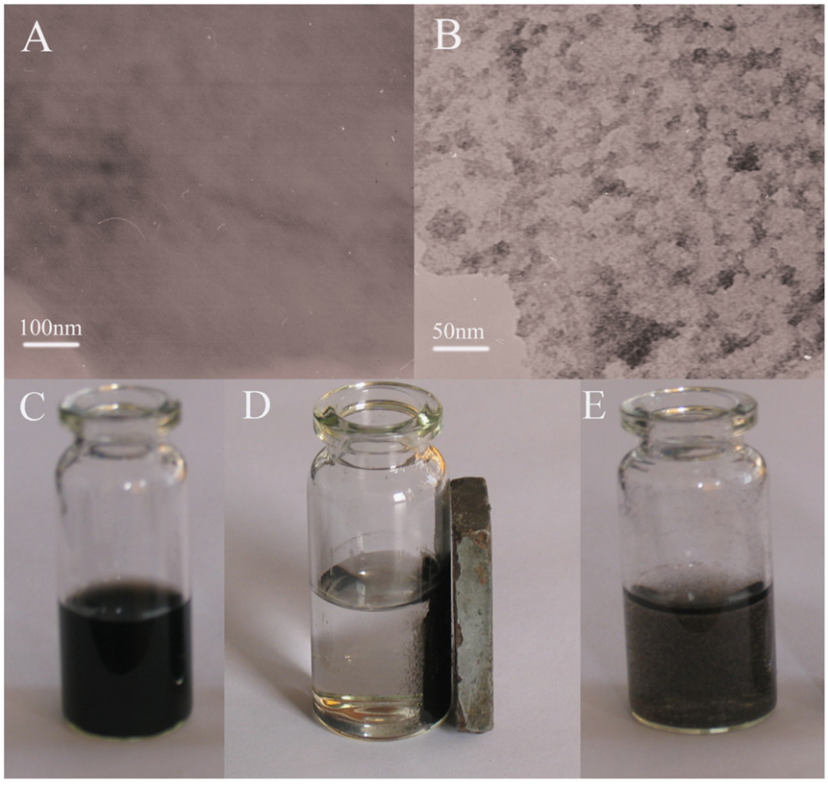

Fig. 1. Characterization of synthesized G@Fe_3O_4: representative TEM images of graphite (A), and G@Fe_3O_4 (B), photographs of graphene (C), G@Fe_3O_4 in ethanol separated by a magnet (D), and G@Fe_3O_4 dispersed in ethanol (E).

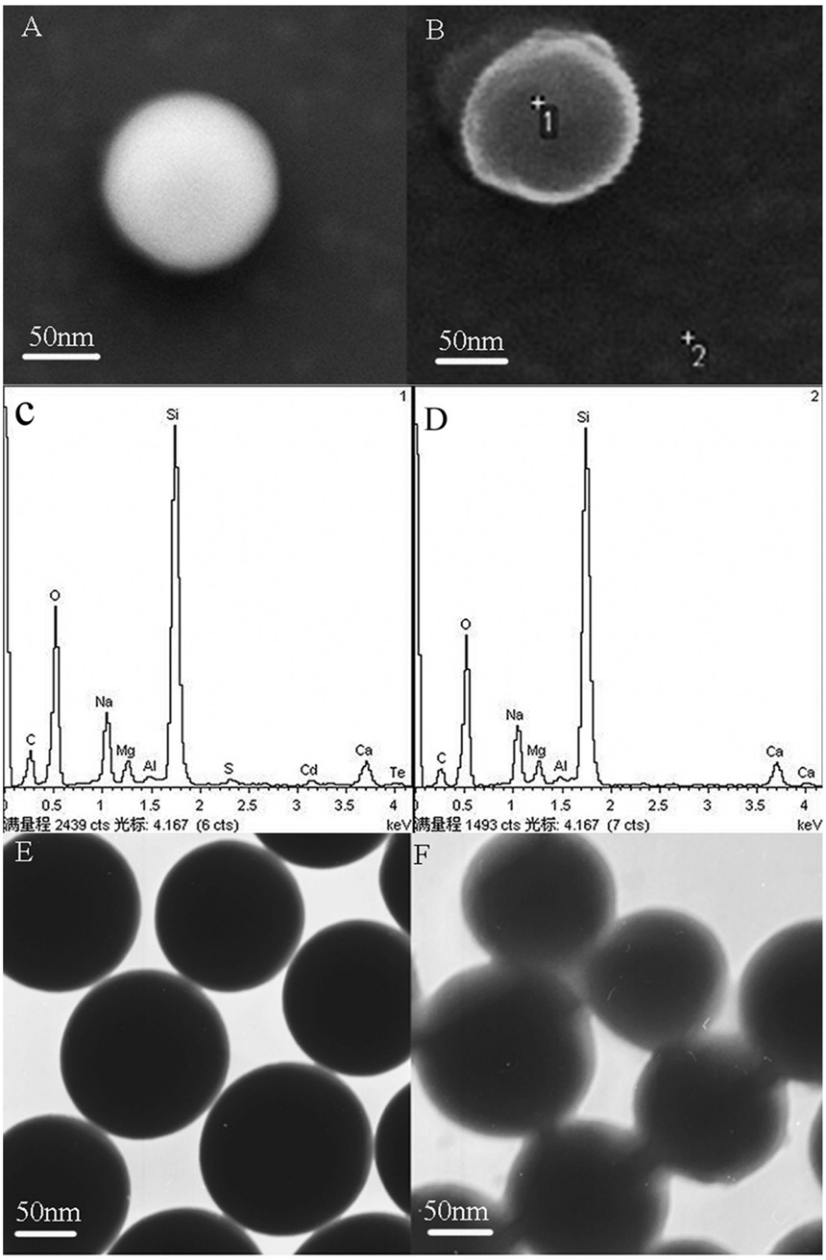

Fig. 2. SEM of silica nanosphere (A), and CdTe QDs functionalized silica nanosphere (B), EDS of CdTe QDs coated silica nanosphere (C,D), and TEM of silica nanospheres (E), and CdTe QDs coated silica nanospheres (F).

showed that the as-prepared silica nanospheres had a chemically clean and homogenized structure with a diameter of 100 ± 5.0 nm (Fig. 2E). The coating of QDs on silica nanospheres was also confirmed by TEM images (Fig. 2F). After the coating process, QDs were deposited on the surface of silica nanospheres, probably in a uniform fashion. All these results confirmed that CdTe QDs had been successfully planted onto the surface of silica nanospheres with excellent dispersivity.

3.4. Comparison of immunoassays using different types of immunosensing probes and different signal labels

To monitor the effect of G@Fe_3O_4 and Si/QDs on the signal amplification of the ECL immunoassay, we prepared two types of immunosensing probes with and without graphene nanosheets (G@Fe_3O_4–Ab_1 and Fe_3O_4–Ab_1), and two types of signal labels for the detection of PSA (the synthesis of Fe_3O_4-Ab_1 was described in Supporting information). The comparison was performed based on the shift of the ECL signal, when the immunosensors were incubated with the 10.0 ng mL^{-1} PSA standard solutions. As seen from Fig. 3A, the G@Fe_3O_4-based immunosensing probe exhibited about 3.2-fold enhancements in ECL signal, compared to Fe_3O_4-Ab_1. The reason might be the fact that the synthesized G@Fe_3O_4 could act as a filterlike network, which could capture more PSA biomolecules than that of the individually dispersed nanoparticles. In contrast to G@Fe_3O_4, the possibility for Fe_3O_4-Ab_1-based immunosensing probe to bind with randomly distributed PSA in the solution might be decreased. The results for Si/QDs and pure CdTe QD as signal labels were listed in Fig. 3B. Using Si/QDs as signal labels showed 4.1-fold in ECL intensity, compared to the pure CdTe QD. This can be explained that the strategy using Si/QDs as signal labels could increase CdTe QDs binding per immunoreaction in comparison with single QD. Therefore, in this work we employ G@Fe_3O_4 as immunosensing probe and Si/QDs as signal labels.

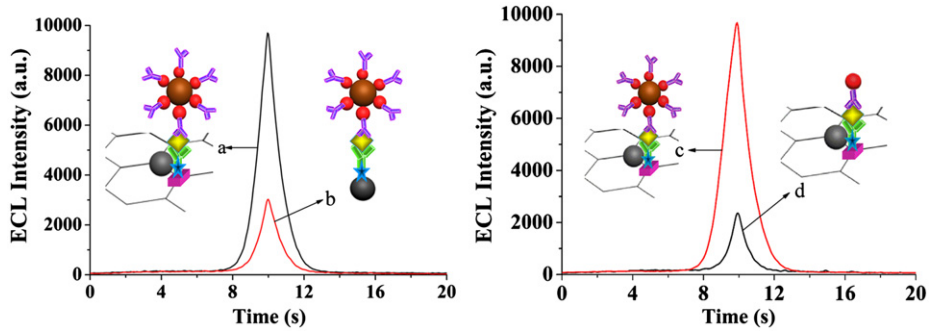

Fig. 3. Comparison of different immunoassays with different immunocomplexes: G@Fe_3O_4/TH–GA–Ab_1–Ag–Ab_2–Si/QDs (a,c), Fe_3O_4/TH–GA–Ab_1–Ag–Ab_2–Si/QDs (b), G@Fe_3O_4/TH–GA –Ab_1–Ag–Ab_2–QDs (d).

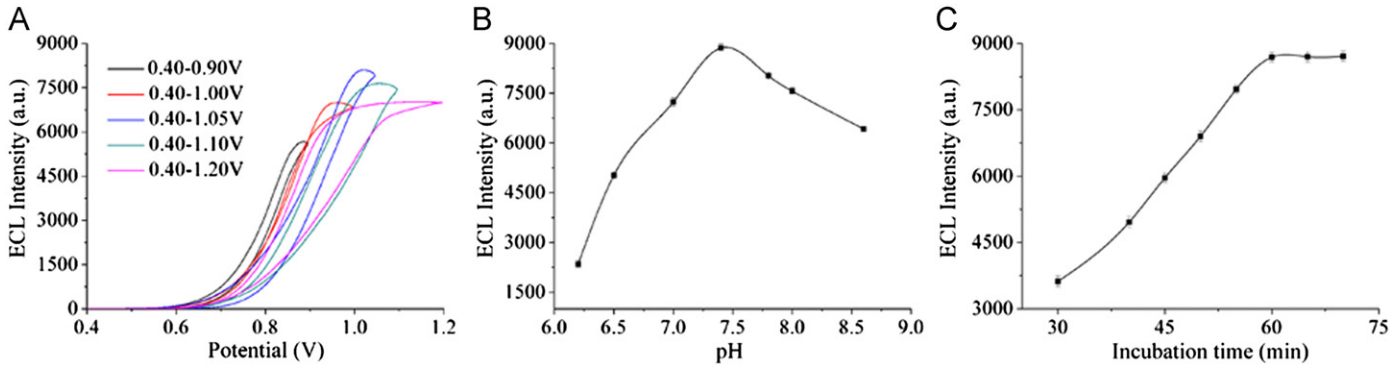

Fig. 4. Effects of potential (A), pH (B) and incubation time (C) on the ECL intensity.

3.5. Optimization of immunoreaction conditions

The ECL intensity of the immunosensor depended on some external conditions to some extent, such as applied potential, pH value and incubation time, so these conditions were selected as follows.

The potential affected the analytical performence in a way, hence different potentials were investigated in our work, and the ECL curves were obtained as the Fig. 4A. It can be observed that the optimal scanning potential was 0.40–1.05 V. According to our knowledge, the chemical properties changed with the pH value, and the ECL intensity of the immunosensor in a different acidity, was shown in Fig. 4B. Obviously, we selected pH∼7.4 as the optimal acidity when the pH value varied from 6.2 to 8.6. Another influencing condition, which cannot be neglected, was the incubation time. As shown in Fig. 4C, the ECL intensity increased with the increasement of the incubation time, and inclined to a constant value after an hour, ascribing to the saturated binding between the analyte and the capture antibody.

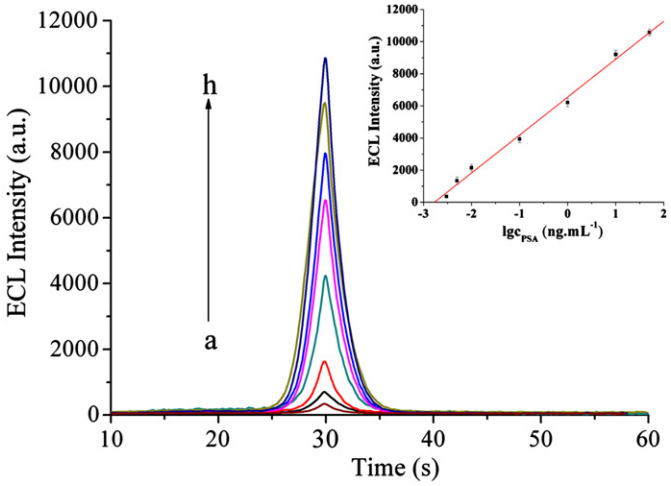

Fig. 5. ECL profiles of the ECL immunosensor in the presence of different concentrations of PSA in PBS containing 0.1 mM Na_2SO_3. Inset: calibration curve for PSA determination. PSA determination (ng mL^{-1}): 0 (a), 0.003 (b), 0.005 (c), 0.01 (d), 0.1(e), 1.0 (f), 10.0 (g), 50.0 (h).

3.6. ECL response of the immunosensor toward PSA standards

Under the optimal condition, the proposed immunosensor was applied to detect the different concentrations of PSA by cyclic voltammetry. The ECL curves of the G@Fe_3O_4/TH–GA–Ab_1–Ag–Ab_2–Si/QDs formed at particular concentrations of PSA were shown in Fig. 5. The ECL intensity corresponding to the blank sample probably was ascribed to the physical adsorption of QDs. Calibration plots displayed a good linear relationship between the ECL intensity and the logarithm of the analyte concentration in the range of 0.003–50 ng mL^{-1} for PSA, and the equation of linear regression was $\triangle$ECL=6548.88+2361.68 lgc$_{PSA}$ (ng mL^{-1}), with a correlation coefficient of 0.9975. The limit of detection (LOD) value for PSA was determined at 0.72 pg mL^{-1}, estimated at a signal-to-noise of 3 criterion, which was partially lower than most of the other immunoassays [27–29].

3.7. Specificity, throughput, reproducibility, and stability of the immunosensor

To confirm that the observed ECL response is generated from the antibody–antigen specific interaction not nonspecific protein interaction, selectivity was investigated when the immunosensor was incubated with the samples containing the following two kinds of potential interfering substances: carcinoma embryonic antigen (CEA, 50 ng mL^{-1}) and human serum albumin (HSA,

50 ng mL^{-1}). Then the ECL response of the mixture was detected through the as-fabracated immunosensor. As shown in Fig. 6, the ECL responses to 10.0 ng mL^{-1} PSA standard solutions with and without interferences showed a difference of less than 5.1%, which suggests that the selectivity of the immunosensor based on the specific antigen-antibody immunoreaction was acceptable.

High sample throughput is a long-cherished goal in the developments of both immunosensor and analyte testing. It is of great significance in early disease diagnosis. To achieve this goal, appropriate analytical time per assay is necessary. The total testing process could be completed within 145 min, including a total incubation time of 140 min for two-step sandwich immunoreaction, 1 min for the ECL signal collection, and washing. Furthermore, parallel incubation could be conveniently performed on several centrifugal tubes, and the ECL detection needed only 1 min, which led to a higher throughput when more centrifugal tubes were used for parallel incubation and immunoassay.

Reproducibility was a vital parameter, too. So we tested it for 10.0 ng mL^{-1} PSA with six fabricated immunosensors independently. The consequence showed a relative standard deviation (RSD) of 4.85%, giving an acceptable fabrication reproducibility of the immunosensors.

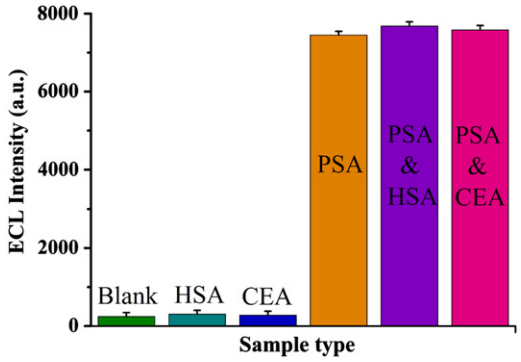

Fig. 6. Specificity of the immunosensor.

Table 1
Comparison of serum PSA levels determined using two methods.

Serum samples	1	2	3
Immunosensor (ng mL^{-1})[a]	90.52	9.68	1.96
ELISA (ng mL^{-1})[a]	96.95	8.93	2.03
Relative deviation (%)	−6.44	7.92	−3.54

Comparison of serum PSA levels determined using two methods.

[a] The average value of three successive determinations.

The stability played vital role in the performance of the prepared immunosensor. After running for 10 cycles (Supporting information Fig. S-3), only a 2.7% decline of the original ECL was observed for G@Fe_3O_4/TH–GA–Ab_1–Ag–Ab_2–Si/QDs, which demonstrated that the sensing layer of the immunosensor posessed excellent stability. Storage stability was also examined by detection of ECL intensity for the as-prepared sensor, and no significant decline was found after 3 weeks of storage at 4 °C, suggesting a good stability of the immunosensor.

3.8. Application of the immunosensor in human serum

The feasibility of applying the immunosensor in clinical systems was investigated by analyzing several real clinical serum samples. The accuracy of PSA determination was examined by comparing the results with those from the enzyme-linked immunosorbent assay (ELISA) analysis. Table 1 shows the correlation results obtained using the proposed immunosensor and the ELISA method. The relative deviations of the proposed immunosensor ranged from −6.44% to 7.92%. It obviously suggested that there was no significant difference between the results given by the two methods. Therefore, the proposed sensor could be reasonably applied in the clinical determination of PSA in human plasma.

3.9. Comparison of analytical properties of different immunoassys toward PSA

For comparison, the analytical properties of the fabricated biosensor were compared with the previously reported PSA biosensors based on utilization of different materials and methods (Table 2). These issues mainly consisted of modified platform, linear range, LOD and detection antibody. These results adequately suggested that the synthesized G@Fe_3O_4 and Si/QDs could greatly improve the sensitivity and working range of the immunoassay.

4. Conclusion

In our work, a sensitive ECL immunosensor for the detection of PSA was developed using biofunctionalized G@Fe_3O_4 as immunosensing probes and Si/QDs as signal amplification labels. G@Fe_3O_4 nanosheets were not only used as a substrate providing a large surface area for the immobilization of biomolecules, but also used to facilitate the rapid separation and purification after synthesis. G@Fe_3O_4 showed the integrated properties of strong superparamagnetism, electrical conductivity, good biocompatibility and excellent processability, so that the subsequent series of composition could be readily attatched on the surface of ITO and could increase the ECL signal without damaging biological structure.

Table 2
Comparison of analytical properties of different immunoassys toward PSA.

Immunoassay format	Modified platform	Signal antibody	Linear range (ng ml−1)	Detection limit (pg ml−1)	Ref.
Electrochemical immunoassay	Single wall carbon nanotube forest	Horseradish peroxidase	1–40	3	[30]
Electrochemical immunoassay	Diaminoheptane-modified nitrocellulose membrane	Quantum dots	0.05–4	20	[31]
Electrochemilumine-scence immunoassay	Graphene	Gold nanorods labeled with glucose oxidase	0.01–8	3	[32]
Electrochemical immunoassay	Single-wall carbon nanotube	Carbon nanotubes- horseradish peroxidase	0.4–40	4	[33]
Electrochemical immunoassay	Screen-Printed carbon electrode array	Multiwalled carbon nanotube	0.005–4	5	[34]
Electrochemilumine-Scence immunoassay	Magnetic Graphene nanosheets	Cdte quantum dots coated silica nanospheres	0.003–50	0.72	This work

Comparison of analytical properties of different immunoassys toward PSA.

And with Si/QDs as labels for signal amplification, a big increase of detection signal was obtained in ECL assay, compared with the unamplified method. In this work, a sandwich-type immunosensor was fabricated to detect PSA for clinical diagnosis through a home-made FI-ECL cell with a very low detection limit, and this proposed method showed accepted specificity, good reproducibility and stability. This sensitive immunoassay is well-suited for high-throughput biomedical sensing and application to other areas.

Acknowledgments

This work was financially supported by Technology Development Plan of Shandong Province, China (Grant no. 2011GGB01153), Natural Science Research Foundation of China (no. 21175058) and Natural Science Foundation of Shandong Province, China (ZR2011BQ019).

Appendix A. Supporting information

Supplementary data associated with this article can be found in the online version at http://dx.doi.org/10.1016/j.talanta.2012.06.021.

References

[1] S.S. Gambhir, Nat. Rev. Cancer 2 (2002) 683–693.
[2] M.S. Wilson, W.Y. Nie, Anal. Chem. 78 (18) (2006) 6476–6483.
[3] D. Ho, K. Falter, P. Severin, H.E. Gaub, Anal. Chem. 81 (8) (2009) 3159–3164.
[4] C.O. Parker, Y.H. Lanyon, M. Manning, D.W.M. Arrigan, I.E. Tothill, Anal. Chem. 81 (13) (2009) 5291–5298.
[5] R.H. Yang, Z.W. Tang, J.L. Yan, H.Z. Kang, Y. Kim, Z. Zhu, W.H. Tan, Anal. Chem. 80 (19) (2008) 7408–7413.
[6] D.P. Tang, R. Yuan, Y.Q. Chal, Anal. Chem. 80 (5) (2008) 1582–1588.
[7] K. Aslan, C.D. Geddes, Chem. Soc. Rev. 38 (9) (2009) 2556–2564.
[8] P.C. Mathias, N. Ganesh, B.T. Cunningham, Anal. Chem. 80 (23) (2008) 9013–9020.
[9] J. Qian, C.Y. Zhang, X.D. Cao, S.Q. Liu, Anal. Chem. 82 (15) (2010) 6422–6429.
[10] Z.P. Chen, Z.F. Peng, Y. Luo, B. Qu, J.H. Jiang, X.B. Zhang, G.L. Shen, R.Q. Yu, Biosens. Bioelectron. 23 (2007) 485–491.
[11] D.P. Tang, J.J. Ren, Anal. Chem. 80 (21) (2008) 8064–8070.
[12] S.S. Zhang, H. Zhong, C.F. Ding, Anal. Chem. 80 (19) (2008) 7206–7212.
[13] W.C. Liao, J.A. Ho, Anal. Chem. 81 (7) (2009) 2470–2476.
[14] I. Willner, E. Katz, Angew. Chem.: Int. Ed. 42 (38) (2003) 4576–4588.
[15] D. Giliohann, C. Mirkin, Nature 462 (2009) 461–464.
[16] M. Green, Angew. Chem.: Int. Ed. 43 (2004) 4129–4131.
[17] Z.X. Zou, D. Du, J. Wang, J.N. Smith, C. Timchalk, Y.Q. Li, Y.H. Lin, Anal. Chem. 82 (12) (2010) 5125–5133.
[18] X.F. Hu, R.Y. Wang, Y. Ding, X.L. Zhang, W.R. Jin, Talanta 80 (3) (2010) 1737–1743.
[19] J. Wang, G.D. Liu, H. Wu, Y.H. Lin, Small 4 (1) (2008) 82–86.
[20] H.J. Kang, M.A. Aziz, B. Jeon, K. Jo, H. Yang, Electroanalysis 21 (24) (2009) 2647–2652.
[21] M.S. Wilson, W.Y. Nie, Anal. Chem. 78 (2006) 2507–2513.
[22] M.S. Wilson, Anal. Chem. 77 (2005) 1496–1502.
[23] H.K. He, C. Gao, Appl. Mater. Interfaces 2 (11) (2010) 3201–3210.
[24] D. Li, M.B. Muller, S. Gilje, R.B. Kaner, G.G. Wallace, Nat. Nanotechnol. 3 (2) (2008) 101–105.
[25] J.B. Joo, Q. Zhang, I. Lee, M. Dahl, F. Zaera, Y.D. Yin, Adv. Funct. Mater. 22 (1) (2012) 166–174.
[26] N. Gaponik, D.V. Talapin, A.L. Rogach, K. Hoppe, E.V. Shevchenko, A. Kornowski, A. Eychmüller, H. Weller, J. Phys. Chem. B 106 (29) (2002) 7177–7185.
[27] E.R. Goldman, G.P. Anderson, J. Conway, L.J. Sherwood, M. Fech, B. Vo, J.L. Liu, A. Hayhurst, Anal. Chem. 80 (22) (2008) 8583–8591.
[28] V.R. Rivera, F.J. Gamez, W.K. Keener, J.A. White, M.A. Poli, Anal. Biochem. 353 (2) (2006) 248–256.
[29] S. Ahn-Yoon, T.R. DeCory, R.A. Durst, Anal. Bioanal. Chem. 378 (1) (2004) 68–75.
[30] B.V. Chikkaveeraiah, A. Bhirde, R. Malhotra, V. Patel, J.S. Gutkind, J.F. Rusling, Anal. Chem. 81 (21) (2009) 9129–9134.
[31] G.D. Liu, Y.Y. Lin, J. Wang, H. Wu, C.M. Wai, Y.H. Lin, Anal. Chem. 79 (20) (2007) 7644–7653.
[32] S.J. Xu, Y. Liu, T.H. Wang, J.H. Li, Anal. Chem. 83 (2011) 3817–3823.
[33] X. Yu, B. Munge, V. Patel, G. Jensen, A. Bhirde, J.D. Gong, S.N. Kim, J. Gillespie, J.S. Gutkind, F. Papadimitrakopoulos, J.F. Rusling, J. Am. Chem. Soc 128 (2006) 11199–11205.
[34] Y. Wan, W.P. Deng, Y. Su, X.H. Zhu, C. Peng, H.Y. Hu, H.Z. Peng, S.P. Song, C.H. Fan, Biosens. Bioelectron. 30 (2011) 93–99.